THE JOURNAL OF PHYSICAL CHEMISTRY B
A JOURNAL OF THE AMERICAN CHEMICAL SOCIETY

pubs.acs.org/JPCB

Article

Ion/Water Network Structural Dynamics in Highly Concentrated Lithium Chloride and Lithium Bromide Solutions Probed with Ultrafast Infrared Spectroscopy

Sean A. Roget, Tristan R. Heck, Kimberly A. Carter-Fenk, and Michael D. Fayer*

Cite This: *J. Phys. Chem. B* 2023, 127, 4532–4543

Read Online

ACCESS | Metrics & More | Article Recommendations

ABSTRACT: The structural dynamics of highly concentrated LiCl and LiBr aqueous solutions were observed from 1−4 to 1−16 water molecules per ion pair using ultrafast polarization-selective pump−probe (PSPP) experiments on the OD stretch of dilute HOD. At these high salt concentrations, an extended ion/water network exists with complex structural dynamics. Population decays from PSPP experiments highlight two distinct water components. From the frequency-dependent amplitudes of the decays, the spectra of hydroxyls bound to halides and to water oxygens are obtained, which are not observable in the FT-IR spectra. PSPP experiments also measure frequency-dependent water orientational relaxation. At short times, wobbling dynamics within a restricted angular cone occurs. At high concentrations, the cone angles are dependent on frequency (hydrogen bond strength), but at higher water concentrations (>10 waters per ion pair), there is no frequency dependence. The average cone angle increases as the ion concentration decreases. The slow time constant for complete HOD orientational relaxation is independent of concentration but slower in LiCl than in LiBr. Comparison to structural MD simulations of LiCl from the literature indicates that the loss of the cone angle wavelength dependence and the increase in the cone angles as the concentration decreases occur as the prevalence of large ion/water clusters gives way to contact ion pairs.

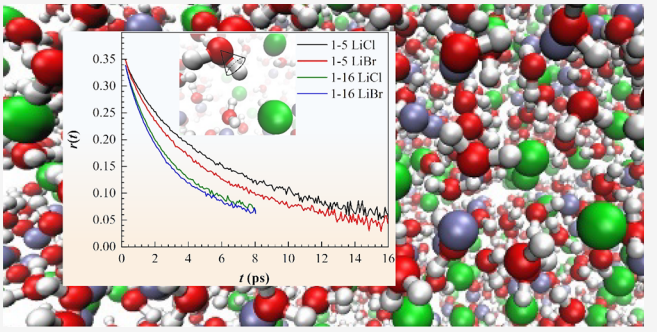

1. INTRODUCTION

Hydrogen bonds (H-bonds) and their dynamics are the source of many of water's remarkable properties, which are critical to many processes in nature and industry. Water is a highly structured but dynamic liquid because of H-bonding, but the presence of solutes, such as ions, can significantly change the physical nature of the liquid. When ion concentration is very high, i.e., there are not enough water molecules to fully solvate individual ions, a complex ion/water network forms. The dynamic structural properties of highly concentrated ionic solutions have important implications for processes in chemistry, biology, and geology.

Bulk water forms an approximately tetrahedral network of H-bonds, having an oxygen atom that can accept 2 H-bonds and two hydroxyls that can donate two H-bonds (up to 4 H-bonds formed per molecule).[1−3] Due to the strength of the interactions, the H-bonds are labile, with the network constantly reorganizing on a ∼2 ps time scale at ambient temperatures.[4−7] Ions are generally very soluble in water and can perturb both the structure and dynamics of the H-bond network. X-ray and neutron diffraction studies aided by theoretical simulations have shown that water molecules rearrange near ions such that their molecular dipoles point toward cations, and water hydroxyls point toward an anions. In essence, hydroxyls form an H-bond to anions.[8−10] Ionic solution dynamics have been studied extensively using experimental methods such as dielectric relaxation,[11] NMR,[12] and ultrafast IR spectroscopy.[6,13−15] Molecular dynamics (MD) simulations have provided a dynamical framework to understand water molecular reorientation near charged species.[16−18]

Highly concentrated salt solutions have been a focus of current research with recent successes with energy storage devices that use "water-in-salt" electrolytes.[19−21] These electrolytes have shown anomalously high Li^+ ion mobility and electrochemical stability for an aqueous electrolyte and with further development could prove to be a safer, environmentally friendly, alternative to organic electrolytes. A topic of debate has been the structural organization of water

Received: December 15, 2022
Revised: April 4, 2023
Published: May 12, 2023

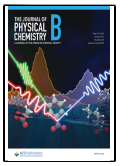

molecules and ions at the high concentration limit, where ion pairs and aggregates are abundant and form extended ion/water networks.[22−24] The structure and dynamics of these ion networks are believed to be a critical factor for understanding ion mobility in these electrolytes, which is required to make effective energy storage devices.

Ultrafast IR spectroscopy can measure time-resolved dynamics, allowing the observation of distinct time scales contributing to orientational relaxation and structural evolution. Probing the OD stretch of dilute HOD in aqueous salt solutions with polarization selective pump−probe (PSPP) experiments can provide a detailed picture of water orientational dynamics and structural information in the form of angular restriction. Recent experiments on highly concentrated LiCl solutions gave details of steric hindrance experienced by water molecules caused by ionic structuring.[15] It was found that water molecules in strong H-bonding configurations experienced more restriction as the salt concentration increased. Time-resolved vibrational relaxation, also measured with PSPP experiments, provided spectroscopic information that cannot be obtained from FT-IR spectroscopy. It was possible to separate the spectra of the hydroxyls (ODs) into water−water and water−anion spectra. These results not only showed that the water-halide H-bonding is weaker than water−water H-bonding, which has been reported in previous studies,[25,26] but also that the water−water H-bonds in the highly concentrated LiCl solutions were, on average, stronger than the H-bonds in bulk water. These observations highlighted novel aspects of water in a system where its H-bond network is heavily disrupted.

In this paper, we extend the previous study in two directions. First, we compare concentrated LiCl and LiBr solutions. In addition, we extend the concentration range to lower ion concentrations, although still highly concentrated. In the study of LiCl, we examined concentrations of 1−4 to 1−6.[15] At these concentrations, there are too few water molecules to form even one solvation shell. Here, for both LiCl and LiBr, we go down to a concentration of 1−16, which contains ∼3.5 M ion pairs (or 7 M ions) and a sufficient number of water molecules to numerically form a complete hydration shell. The spectroscopic and dynamic experimental results are very similar for the LiCl and LiBr solutions, although there are some distinct differences.

While the FT-IR spectra of the OD stretch of HOD in the solutions are single bands, the spectra obtained from the PSPP experiments, the Lifetime Amplitude Spectra (LAS), give the spectra of ODs bound to halide anions and ODs bound to water oxygens. The bands are shifted to higher frequencies for the LiBr solutions compared to the LiCl solutions. At the highest concentrations, the areas of the spectra show that there are far more hydroxyls bound to halide anions than to water oxygens. However, at 1−16 concentration (increased water concentration), there are significantly more ODs H-bonded to other water molecules than to halide anions. At each concentration, the hydroxyls bound to halide anions/hydroxyls bound to water ratio are identical for LiCl and LiBr within error.

Water orientational relaxations in the two salt solutions from the PSPP measurements are also very similar. The anisotropy decays have two components. The fast component of the decays is caused by wobbling-in-a-cone dynamics, i.e., restricted angular sampling over a limited range of angles, the cone angles.[27−30] At the highest concentrations, the cone angle is frequency-dependent. This dependence is well described by a linear fit, and the slope of the line decreases with increasing water concentration. At a concentration of 1−10, there is no longer a frequency dependence. As the water concentration increases, the average cone angle also increases. However, in pure water, the wobbling cone is negligible. Therefore, at some higher water concentration, above 1−16, the cone angle is likely to decrease. These experiments present an intriguing view of the structural dynamics and structure of these highly concentrated water-salt solutions.

2. EXPERIMENTAL METHODS

2.1. Sample Preparation. Anhydrous LiCl and LiBr salts (>99%) were used as received from Sigma-Aldrich. To ensure that the salts remained dry prior to use, they were stored in a dry glovebox continuously purged of moisture. To perform the nonlinear experiments, aqueous salt solutions of varying molar ratios (1−4, 1−5, 1−6, 1−10, 1−16) were prepared using 5% HOD in H_2O. HOD is an excellent probe of water dynamics as the OD stretch provides a local vibrational mode distinct from the OH stretch region of bulk water.[31] At 5% molar concentration, HOD is sufficiently dilute to avoid resonant transfer of vibrational energy between molecules and has a negligible effect on the structure and properties of H_2O.[4,5,32,33] The salt solutions were sandwiched between two CaF_2 windows using a 12 μm spacer to set the path length. A Thermo Scientific iS50 FT-IR spectrometer was used to measure linear IR absorption spectra of the samples (at 0.5 cm^{-1} resolution). To isolate the linear spectrum of the OD stretch, spectra of salt solutions prepared with neat H_2O were also taken and used for background subtraction. Each nonlinear experiment was run three times, and fresh samples were prepared for each run.

2.2. Laser System and Nonlinear Experiments. The laser system used to perform the nonlinear IR experiments has been described previously in detail.[34] In summary, a regenerative amplifier system, seeded by a Ti:Sapphire oscillator, was used to pump an optical parametric amplifier (OPA). The OPA output was then difference frequency mixed in a $AgGaS_2$ crystal to generate mid-infrared (mid-IR) pulses that were centered at ∼4 μm with a pulse duration of ∼65 fs. The pulses were then split into 2, pump and probe, beams, and were crossed in the sample to generate a nonlinear signal. The timings of the pulses were controlled using precision delay stages. The experiments were frequency-resolved by a spectrograph equipped with a 32-pixel mercury-cadmium-telluride array detector.

In the PSPP experiments, the mid-IR was split into a strong pump and weak probe pulse. The probe was horizontally polarized (0°), and the pump pulse was polarized +45° relative to the probe. A computer-controlled polarizer after the sample resolved the probe (and signal) either parallel (+45°) or perpendicular (−45°) to the pump. To avoid polarization bias from the diffraction grating, a second polarizer before the monochromator set the polarized signal to be horizontal (0°). The parallel, $S_{\parallel}(t)$, and perpendicular, $S_{\perp}(t)$, signals were then analyzed to determine the population relaxation, $P(t)$, and anisotropy, $r(t)$, according to the equations

$$P(t) = \frac{1}{3}[S_{\parallel}(t) + 2S_{\perp}(t)] \quad (1)$$

https://doi.org/10.1021/acs.jpcb.2c08792
J. Phys. Chem. B 2023, 127, 4532−4543

$$r(t) = \frac{S_{\parallel}(t) - S_{\perp}(t)}{S_{\parallel}(t) + 2S_{\perp}(t)} = 0.4C_2(t) \quad (2)$$

where $C_2(t)$ is the second-order Legendre polynomial orientational correlation function. An additional long-lived isotropic signal arises from vibrational relaxation of the excited OD stretch dissipating as heat into the chemical system. A well-documented procedure was used to remove this heating signal for accurate determination of the dynamics of interest.[7,35]

3. RESULTS AND DISCUSSION

3.1. Linear Spectra. The linear spectra of the OD stretch of HOD were measured in bulk water and various concentrations of LiBr and LiCl solutions, as shown in Figure 1. The OD stretch vibrational mode is sensitive to the diverse

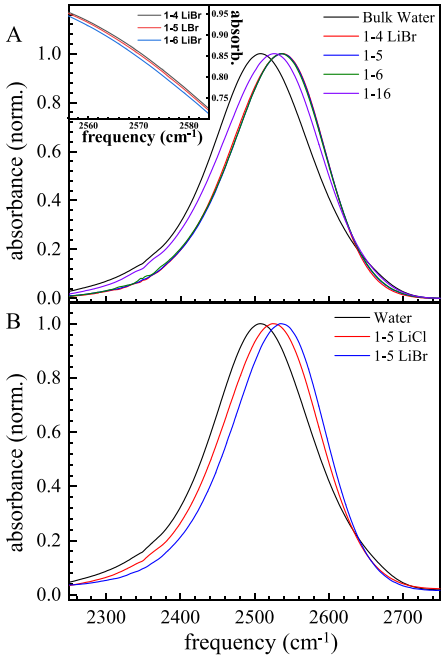

Figure 1. Background-subtracted and normalized linear absorption spectra of the OD stretch of HOD in bulk water and (A) in aqueous LiBr solutions of molar ratios, 1−4, 1−5, 1−6, and 1−16 (water molecules per ion pair) and (B) in aqueous LiCl and LiBr solutions at a 1−5 molar ratio. The inset shows the small change for the concentrations 1−4 through 1−6.

H-bonding configurations present in the H-bond network. As a result, the vibrational mode is significantly inhomogeneously broadened in bulk water with a FWHM of ∼160 cm^{-1}. When salts are dissolved to form an aqueous solution, the shape and center position of the linear spectra are modified by water−ion H-bonding interactions. The concentration dependence of the linear spectra in LiBr solutions is shown in Figure 1A. The linear spectrum shifts toward higher frequencies with the addition of the lithium halide salts. While both the cation and anion play a role in the modification of the H-bond network, water−anion interactions have a dominant impact on the linear spectrum of the OD stretch.[13,36,37] Water molecules that are in weaker H-bonding configurations contribute to the high frequency side of the absorption line shape.[38] In some cases, the water−anion H-bond interaction can be spectrally distinct from water−water interactions when there is a large difference in H-bond strength.[39−41] The spectra in Figure 1 indicate that the water−halide interactions present in solution are weaker than the average H-bond in bulk water because of the frequency shift to higher frequencies with increasing salt concentration. In Figure 1B, the linear spectra of the OD stretch in LiBr and LiCl solutions are shown for the same molar ratio of 5 water molecules per ion pair (1−5). The spectrum is centered at a higher frequency in LiBr (2535 cm^{-1}) when compared to LiCl (2525 cm^{-1}) at the same concentration; this implies that the water−bromide H-bonds are weaker than water−chloride H-bonds. The decreased charge density of Br^- leads to a weaker interaction between the ion and the water hydroxyl bond compared to Cl^-.[25]

The OD stretch spectrum in bulk water is asymmetric due to the frequency-dependent transition dipole moment that is associated with H-bonding interactions, i.e., the non-Condon effect.[42,43] The transition dipole of the OD stretch has a larger magnitude for hydroxyls in strong H-bonding configurations. These hydroxyls absorb at lower frequencies, resulting in the characteristic red-wing of the absorption line shape. In the salt solutions, the spectrum is even more asymmetric due to contributions from two distinct ensembles; that is the water-associated population, where the OD bond of HOD donates an H-bond to another water oxygen, and the anion-associated population, where the OD bond donates an H-bond to an anion. This effect can be seen in Figure 1A by the shift of the linear spectrum of HOD in LiBr as more salt is added to the solution, and water−bromide interactions become more common. At very high LiBr concentrations, the spectra are almost, but not quite identical (see inset Figure 1A). Both components of the spectra are affected by the non-Condon effect; therefore, the total spectrum observed through FT-IR spectroscopy is the sum of two spectra that deviate from Gaussians at lower frequencies. For this reason and due to the relatively small shift between the peak centers compared to the linewidths, distinguishing the various H-bonding interactions present in the linear spectra through peak fitting is not possible. In the next section, we describe how we can use nonlinear IR experiments to separate these contributions.

3.2. Population Relaxation. The distinct water interactions can be resolved using the population relaxation measured in the PSPP experiments (eq 1).[13,15,23,44−46] The excited-state lifetime of the OD stretch is sensitive to local interactions of the water molecules. The time constant is a result of the coupling of vibrational energy in the excited state to intramolecular modes of HOD and to the continuum of intermolecular low frequency bath modes.[47] Depending on the chemical environment, the OD stretch vibrational lifetime can range from a few picoseconds to tens of picoseconds.[13,44,46,48−50] HOD molecules that are in the first solvation shell of anions have a lifetime that is distinct from those outside the first solvation shell. The normalized population relaxation of HOD near 2535 cm^{-1} in bulk water and in LiCl and LiBr solutions at 1−5 molar ratio are shown in Figure 2. The vibrational lifetime of the OD stretch of HOD in bulk water is 1.8 ± 0.1 ps. The population relaxation of HOD in the aqueous salt solutions fits best to a biexponential decay, with the form

$$P(t) = a_1(\omega)e^{-t/t_1} + a_2(\omega)e^{-t/t_2} \quad (3)$$

The biexponential decay demonstrates that there are two distinct ensembles of HOD molecules contributing to the overall pump−probe signal, with amplitudes, a_i, and vibrational

https://doi.org/10.1021/acs.jpcb.2c08792
J. Phys. Chem. B 2023, 127, 4532−4543

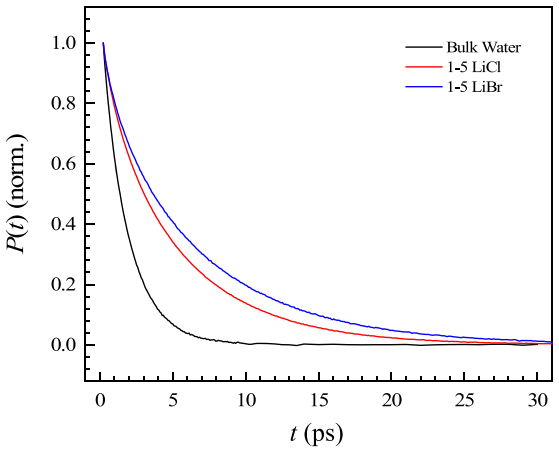

Figure 2. Vibrational population relaxation of the OD stretch of HOD in pure water and in 1−5 LiCl and LiBr aqueous solutions near 2535 cm^{-1}.

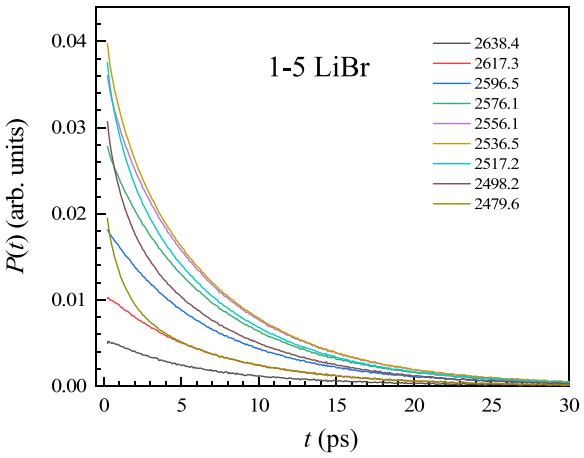

Figure 3. Frequency-dependent population relaxation of the OD stretch of HOD in 1−5 LiBr aqueous solution.

lifetimes, t_i. The two distinct lifetimes are from water−water and water−anion interactions present in the salt solutions. The lifetimes from the biexponential fits as a function of concentration for the halide salt solutions are given in Table 1. There is a fast time constant in both salt solutions that is independent of the anion and similar to that of HOD in bulk water; this is the water-associated population of ODs present in the solutions. The slow time constant observed from the fits is dependent on the anion and roughly varies with concentration; this is the anion-associated population of ODs. Interactions with bromide anions result in a slightly longer lifetime compared to chloride anions. This assignment is consistent with prior experiments in which there is sufficient difference in the spectra (OD stretch of HOD) of the water−water and water−anion species to assign the bi-exponential decays to the different species. In an aqueous solution of BF_4^-, the water−water and water−anion lifetimes are 2.2 and 9.4 ps, respectively.[40] In AOT reverse micelles the water−water lifetime is 1.8 ps, while the lifetime of water H-bonded to the sulfonate head groups of the AOT surfactants is 4.5 ps.[51]

Table 1. Observed Vibrational Lifetimes from Fits to the Population Relaxation of the OD Stretch of HOD in Aqueous Lithium Halide Solutions[a]

solution	t_w (LiCl)	t_w (LiBr)	t_a (LiCl)	t_a (LiBr)
1−4	1.3 ± 0.1[b]	1.4 ± 0.1	6.4 ± 0.1[b]	8.1 ± 0.2
1−5	1.1 ± 0.1[b]	1.2 ± 0.1	5.5 ± 0.1[b]	7.0 ± 0.1
1−6	1.0 ± 0.1[b]	1.1 ± 0.1	5.3 ± 0.1[b]	6.2 ± 0.2
1−16	1.8 (fixed)	1.8 (fixed)	4.3 ± 0.1	3.7 ± 0.1

[a] t_w: lifetime of the water-associated population; t_a: lifetime of the anion-associated population. [b] reproduced from ref 15.

The linear spectra highlighted that the anion-associated population is shifted to higher frequencies compared to the water-associated population. The population relaxation of HOD in the aqueous salt solutions is therefore frequency-dependent, as the relative contribution of each ensemble varies across the absorption line shape. The frequency dependence of the population decays (not normalized) are shown for LiBr at a 1−5 molar ratio in Figure 3. The frequency-dependent amplitudes, $a_i(\omega)$, from the biexponential fits are the water-associated and anion-associated amplitudes of the decays at a given frequency. Plotting these amplitudes as a function of frequency gives spectra of the two components, i.e., the LAS. Because of the high quality of the data, the error bars on the $a_i(\omega)$ used to plot the LAS are < $\pm 10^{-4}$.

LAS reveal information that is not resolvable in the linear spectra. The concentration dependence of the LAS for some of the LiBr solutions is shown in Figure 4. The concentrations 1−4 to 1−6 are essentially the same. The bromide-associated component is shifted to higher frequencies compared to bulk water (2510 cm^{-1}). It is centered at 2544 ± 0.3 cm^{-1}, while the water-associated component is shifted to lower frequencies, centered at 2498 ± 0.4 cm^{-1} (see dashed arrows). The spectra are limited at lower frequencies because of overlap between the 0−1 and 1−2 transitions observed in the third-order nonlinear experiments. The position of the anion-associated component highlights the weaker H-bond that forms between water and the anion.

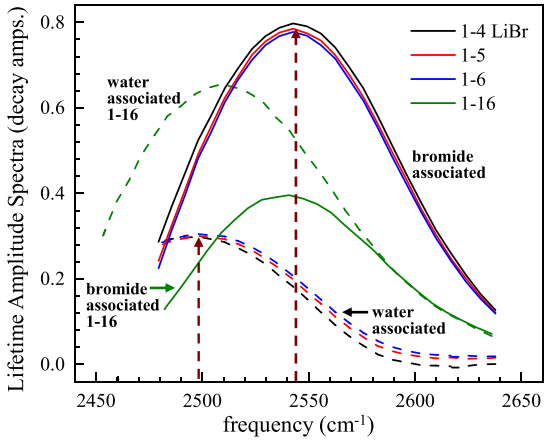

Figure 4. Frequency-dependent population amplitudes, a_i, of hydroxyls (ODs) H-bonded to water oxygens (dashed lines) and bromide anions (solid lines) determined from the population decays at each frequency (Lifetime Amplitude Spectra). The sum of the two component spectra gives the normalized, isotropic pump−probe spectrum. The vertical dashed arrows are the center frequency of the two components for the concentrations 1−4 through 1−6.

A comparison of the LAS for LiBr and LiCl solutions at the 1−5 molar ratio is shown in Figure 5. Like the LAS for LiBr, the LAS for LiCl for concentrations 1−4, 1−5, and 1−6 are

https://doi.org/10.1021/acs.jpcb.2c08792
J. Phys. Chem. B 2023, 127, 4532−4543

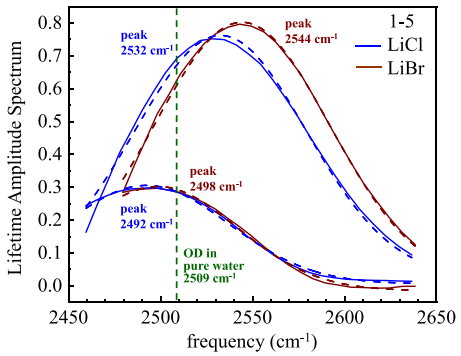

Figure 5. Comparison of the Lifetime Amplitude Spectra (solid curves) of LiCl and LiBr solutions for concentration, 1−5. The dashed curves are Gaussian fits to the data. The vertical dashed green line shows the peak frequency of pure water.

almost the same. Gaussian fits (dashed lines) are quite good given the manner in which the LAS were acquired. Peak frequencies and areas of each peak were obtained from the Gaussian fits like those shown in Figure 5 for all concentrations. The OD of water molecules H-bonded to bromide absorb at higher frequency compared to those H-bonded to chloride. The peak frequencies are 2544 ± 0.3 and 2532 ± 0.6 cm^{-1} for Br^- and Cl^-, respectively. The shift to higher frequency for Br^- is caused by a decrease in charge density between the two anions.

As observed previously in highly concentrated LiCl solutions,[15] and as can be seen in Figure 5 for both LiCl and LiBr, the water-associated component is shifted to lower frequencies compared to the bulk water spectrum, which is centered at 2509 cm^{-1} (green dashed line). The OD−water interaction shifts the OD stretch further to lower frequency in the LiCl solutions compared to the LiBr solutions. The average H-bond strength of the hydroxyl−water interaction is indirectly affected by the presence of ions. Since cations act in a manner like H-bond donors, i.e., they associate with oxygen lone pairs, water−lithium interactions do not have a strong influence on the lifetime and, therefore, do not appear in the LAS as a separate component. The influence of water−lithium interactions appear in the hydroxyl−water associated population. Li^+ bound to the oxygen lone pair of an HOD will withdraw electron density from the oxygen. The reduced electron density will in turn cause the oxygen to withdraw additional electron density from the deuterium. The deuterium will have a larger positive partial charge, δ^+, compared to an HOD in pure water. These deuterium atoms with increased δ^+ will form stronger H-bonds to water oxygens than those in pure water. MD simulations have also shown that water−water interactions that occur in the first and second solvation shells of ions can experience enhanced H-bond strength due to the electrostatic ordering of water molecules.[52] Specifically, the electrostatic ordering induced by an ion on its first solvation shell aligns a water molecule in a manner that strengthens/shortens its H-bond to another water molecule in the second solvation shell. Notably, this effect is more significant for water in the first solvation shell of a cation (compared to an anion) and ions with higher charge density. These factors demonstrate how the presence of Li^+ contributes to the red shift of the OD−water interaction.

The separation of the pump−probe spectrum into its component spectra using the LAS method also provides information on the relative number of hydroxyl−water interactions and hydroxyl−anion interactions present in the aqueous salt solutions. The ratios of interactions are determined from the relative areas of Gaussian fits to the component spectra. Because of the overlap of the 1−2 transition with the 0−1 transition's red side, the red sides of the LAS plotted in Figures 4 and 5 are not accessible. The Gaussian fits do not capture the red tails of the spectra (see Figure 1), which arise from the non-Condon effect.[42,53] The non-Condon effect is the variation in the transition dipole with frequency. For water systems, as the frequency is reduced, the transition dipole increases. However, the deviation from a Gaussian line shape in the absorption spectra, for which the entire spectrum can be measured, is not large. Fitting the water absorption spectrum to a Gaussian on the blue side of the line to somewhat past the peak, and comparing the resulting Gaussian area to the total area shows that the red tail is only ∼5% of the spectrum. Then, in dividing the Gaussian fits for the two components, an error will occur, which depends on the difference in true areas caused by the tails from those obtained from the Gaussian fits. If one component Gaussian fit is 0.95 of the true area and the other is 0.9 of the true area (a very large difference), the error is small, ∼5%. It should also be noted that the red tail is caused by an increase in the transition dipole, not an increase in concentration. Vibrational line shapes in liquids are generally Gaussian in the absence of a frequency-dependent transition dipole. In bulk water, missing the area in the red tail is not missing a significant fraction of the absorption line. It seems likely that the same considerations apply to the components of the LAS. It is the ratio of the concentrations that is the desired quantity. A detailed simulation[54] has shown that the distribution of frequencies associated with all H-bond strengths in water, without transition dipoles, is Gaussian. Therefore, using a Gaussian fitting function to determine the relative areas should not introduce significant error.

From the Gaussian fits (see example in Figure 5), in combination with the concentration dependence, this information provides an interesting picture on how the ion network evolves as the water concentration is increased. The concentration dependence of the ratio of the areas for the H-bonding of hydroxyl−anion to hydroxyl−water populations is given in Table 2. The ratios are essentially within error of each other for the two salt solutions. The results imply that the number of hydroxyls coordinated to chloride or bromide anions are the same, even though the bromide anion is somewhat larger, in agreement with X-ray techniques and complementary MD simulations. These studies indicate that the number of water molecules coordinated to chloride and

Table 2. Fraction of Hydroxyls (ODs) H-Bonded to Halides to Hydroxyl H-Bonded to Water Oxygens in Aqueous Lithium Halide Solutions for Various Concentrations (Ion Pair-Water Molecules)

solution	LiCl ratio (OD···Cl/OD···O)	LiBr ratio (OD···Br/OD···O)
1−4	3.4 ± 0.2	3.4 ± 0.2
1−5	3.4 ± 0.2	3.6 ± 0.2
1−6	2.7 ± 0.2	3.0 ± 0.2
1−7	2.8 ± 0.2	2.1 ± 0.2
1−10	1.0 ± 0.1	1.0 ± 0.1
1−16	0.52 ± 0.05	0.52 ± 0.05

https://doi.org/10.1021/acs.jpcb.2c08792
J. Phys. Chem. B 2023, 127, 4532−4543

bromide anions are nearly identical, ranging from 6−8 water molecules, while 4 water molecules are coordinated to a lithium ion.[8,10,55] At the highest salt concentrations, there are not enough water molecules to fully solvate both cations and anions without having overlapping solvation shells. In fact, MD simulations show that there is significant ion pairing present in solution at these concentrations.[56−58] From the LAS measurements, there is no change in the ratios as the water content goes from 1−4 to 1−5. For 1−6 and 1−7, the ratios have changed slightly, but the really dramatic change comes at 1−10. For 1−4, there are more than 3 times as many hydroxyls H-bonded to a halide anion than to a water oxygen. At 1−10, there are just as many hydroxyl−water interactions as there are hydroxyl−halide interactions. As the water concentration continues to increase, i.e., 1−16, there are twice as many hydroxyls H-bonded to other water molecules than to halide anions. At 1−16, there are more water molecules than are necessary to solvate the ions, and an extended water−water network is beginning to form. Because of the likely error introduced by using Gaussians to fit the LAS (see Figure 5), the error bars on the ratios given in Table 2 are somewhat larger than 5% for the higher ion concentrations and about 10% for the lower ion concentrations. However, the large changes in ratios of the highest ion concentrations to lower ion concentrations are not obscured by the error bars.

While the ratios given in Table 2 are informative, it is important to recognize that in addition to hydroxyls H-bonding to halides and to other water molecules, there are also non-H-bonded hydroxyls. In pure water, H-bonds are constantly dissociating and reforming. In this process, hydroxyls are not H-bonded for less than a few hundred femtoseconds.[59] Although a non-H-bonded hydroxyl quickly forms an H-bond, ∼one eighth of the hydroxyls are not H-bonded at any instant. In the crowded concentrated ionic solutions studied here, in addition to the fleeting non-bonded hydroxyls there will also be hydroxyls unable to H-bond because of geometry mismatching, which does not occur in pure water. These may also be short-lived, but these hydroxyls are likely to remain non-H-bonded for longer than those in pure water. Hydroxyls that are not H-bonded have a significantly smaller transition dipole than H-bonded hydroxyl, approximately a factor of two smaller, and their spectrum will be shifted to higher frequency, ∼2700 cm^{-1}.[60] The signal in the pump−probe experiment that provides the LAS depends on the 4th power of the transition dipole. The small transition dipole will make the ensemble of non-bonded hydroxyls invisible to the pump−probe experiment, and therefore, its contribution to the LAS is negligible. As the water concentration is changed, the fraction of hydroxyls that are non-H-bonded will change.

The presence of non-H-bonded hydroxyls in complex solutions is supported by experiments and simulation from Maroncelli and co-workers. Isolated water molecules in room temperature ionic liquids and polar solvents were studied using FT-IR spectroscopy. Evidence was presented indicating that in addition to both hydroxyls of water molecules forming H-bonds, some waters made only one H-bond and had a non-H-bonded hydroxyl.[61,62]

These LAS observations highlight that, at high concentrations (1−4 through 1−7), as the amount of water is increased, the ion network reorganizes in a manner that does not dramatically change the relative ratios of hydroxyls H-bonded to a halide and to another water until there are sufficient water molecules (∼1−10) to form a more extended water network. Exact configurations of these anion−cation, water−anion, and water−cation as well as water−water interactions are difficult to establish from experiments alone. However, these relative ratios provide experimental details that can corroborate MD simulations, which could provide structures of these highly concentrated systems.

3.3. Orientational Dynamics. The orientational relaxation of HOD molecules in concentrated halide salt solutions was observed through the anisotropy, $r(t)$, calculated from the time-dependent PSPP signals using eq 2. For a single ensemble of HOD molecules, the anisotropy is proportional to the orientational correlation function, $C_2(t) = \langle P_2(\hat{\mu}(0) \cdot \int \hat{\mu}(t))\rangle$, where P_2 is the second-order Legendre polynomial function, $\hat{\mu}(t)$ is the unit vector of the transition dipole moment at time, t, and $\langle ...\rangle$ denotes an ensemble average over all molecules contributing to the nonlinear signal. The anisotropy of HOD in bulk water decays as a single exponential with a reorientation time constant of 2.6 ps.[6,7] Water molecules in the bulk liquid undergo orientational relaxation through jump reorientation, a concerted mechanism involving large angular motions (∼60°) in which water molecules break and rapidly reform the extended H-bond network.[63,64] MD simulations have used the extended jump model to describe the orientational dynamics in a wide range of aqueous systems, including in the solvation shells of ions.[16,18,65,66]

The anisotropy decays, $r(t)$, of HOD in lithium halide salt solutions are shown in Figure 6. $C_2(t)$ takes on a maximum

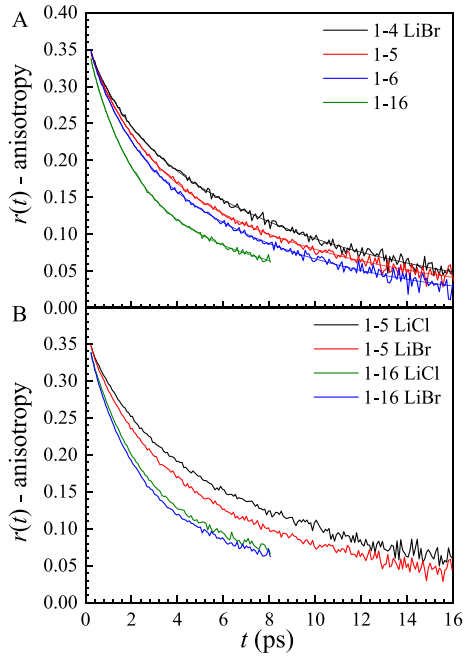

Figure 6. (A) Anisotropy decays of the OD stretch of HOD in aqueous LiBr solutions for concentrations, 1−4, 1−5, 1−6, and 1−16 near 2535 cm^{-1}. (B) Comparison of anisotropy decays in LiCl and LiBr solutions at concentrations 1−5 and 1−16 near 2535 cm^{-1}.

value of 1 at t = 0, when the directions of the OD transition dipoles have an initial $\cos^2\theta$ angular distribution; therefore, $r(0)$ = 0.4 (eq 2). However, ultrafast inertial motions contribute to the orientational relaxation. These occur in <100 fs and cannot be resolved due to the duration of the mid-IR pulses.[67] Thus, when the anisotropy decays are fit, $r(0)$ is

https://doi.org/10.1021/acs.jpcb.2c08792
J. Phys. Chem. B 2023, 127, 4532−4543

below 0.4. The amplitude of the inertial component can be quantified by the difference between 0.4 and the experimentally observed value at $t = 0$. In Figure 6A, the concentration dependence of the anisotropy for LiBr solutions is shown. In both lithium halide salts, the anisotropy decays faster as the salt concentration is decreased. A comparison of the anisotropy of HOD in LiCl and LiBr at two molar ratios, 5 and 16 waters per ion pair, is shown in Figure 6B. The anisotropy decays somewhat more quickly in the LiBr solutions than in LiCl.

The anisotropy decays in both halide salt solutions fit best to a biexponential decay, indicating that there are two processes contributing to water reorientation. For the population relaxation in the previous section, two distinct ensembles for the OD lifetime were identified. The lifetime is very sensitive to the species to which the OD is H-bonded, i.e., a halide or a water oxygen. However, orientational relaxation will involve interactions of the HOD molecule with surrounding ions and water molecules, e.g., if the OD is H-bonded to bromide, the OH can be H-bonded to a water oxygen.[16,18,65,66] The orientational relaxation will be determined by all of the interactions of HOD with its surroundings. Therefore, HOD orientational relaxation occurs as a single ensemble.

For salt solutions,[13,14] the two processes contributing to the orientational dynamics can be described using the wobbling-in-a-cone model. In this model, water molecules undergo restricted angular diffusion at shorter times. Following constraint release, complete angular randomization occurs on the longest time scale.[27−30] The restricted angular diffusion corresponds to motions within an angular volume characterized by a cone of half angle, θ_c. The form of the orientational correlation function that describes the diffusive motions within the cone is given by

$$C_2(t) = S^2 + (1 - S^2)\exp(-t/t_c) \quad (4)$$

where S is the order parameter related to the cone angle by, $S = \frac{1}{2}\cos(\theta_c)[1 + \cos(\theta_c)]$, and t_c is the wobbling time constant. The restricted angular diffusion constant, D_c, can be determined from θ_c and t_c using an approximate form that is accurate for $\theta_c < 30°$[28]

$$D_c \cong \frac{7\theta_c^2}{24t_c}. \quad (5)$$

The full expression described in the literature can be used for $\theta_c > 30°$.[28,68] In the salt solutions, water molecules also sample all angles on the longest time scale, so the total orientational correlation function that is observed through the anisotropy, including the inertial motions, is given by[68]

$$C_2(t) = T^2[S^2 + (1 - S^2)\exp(-t/t_c)]\exp(-t/t_m) \quad (6)$$

where T is the order parameter for the ultrafast inertial decay and t_m is the free diffusion time constant for complete randomization, which is related to the angular diffusion constant, D_m ($t_m = 1/6D_m$).

The biexponential fits to the anisotropy (Figure 6A) yield two time constants, t_1 and t_2 ($t_1 < t_2$), that are related to the time constants in the wobbling-in-a-cone model, $t_c = (t_1^{-1} - t_2^{-1})^{-1}$ and $t_m = t_2$. The diffusion constants and time constants are given in Table 3 for both halide salts over a range of concentrations. Within experimental error, the time constants are insensitive to changes in the salt concentration over the range studied. While the wobbling time constant, t_c, remains the same at ∼2 ps for the two halide salts, the free diffusion time constant, t_m, is faster in the bromide solutions (9 ps) compared to the chloride solutions (∼11 ps). For both solutions, the complete orientational relaxation is much slower than bulk water (2.6 ps).

Table 3. Fit Parameters for the Anisotropy of the OD Stretch of HOD in Bulk Water and Aqueous LiCl Solutions Using Wobbling-in-a-Cone Analysis for Restricted Orientational Relaxation

solution	t_1	t_c	D_c^{-1} (ps)[a,b]	θ_c[a]	$t_m = t_2$ (ps)	D_m^{-1} (ps)
LiCl 1−4[c]	1.6 ± 0.2	1.9 ± 0.2	34 ± 6	26	12 ± 1	72 ± 6
1−5[c]	1.6 ± 0.1	2.0 ± 0.2	30 ± 4	28	10 ± 1	60 ± 6
1−6[c]	1.8 ± 0.1	2.2 ± 0.2	28 ± 1	32	11 ± 1	66 ± 6
1−16	1.8 ± 0.1	2.2 ± 0.2	16 ± 1	43	12 ± 1	72 ± 6
LiBr 1−4	1.5 ± 0.1	1.8 ± 0.2	29 ± 6	28	9 ± 1	54 ± 6
1−5	1.6 ± 0.2	2.0 ± 0.2	28 ± 3	30	9 ± 1	54 ± 6
1−6	1.8 ± 0.1	2.2 ± 0.2	25 ± 1	34	9 ± 1	54 ± 6
1−16	1.7 ± 0.1	2.0 ± 0.2	16 ± 1	41	9 ± 1	54 ± 6
bulk water					2.6 ± 0.1	15.6 ± 0.6

[a]Average across all frequencies. [b]Error bars are the standard deviation across all frequencies. [c]Reproduced from ref 15.

The frequency-averaged cone angles are also provided in Table 3. Differences in θ_c and t_m contribute to the faster anisotropy decay observed in LiBr solutions (Figure 6B). However, the concentration dependence of the anisotropy in the lithium halide salts (Figure 6A) results solely from changes in θ_c. From Table 3, θ_c increases significantly as the salt concentration decreases. The increase in the cone angle causes the fast component to the anisotropy relaxation to contribute more to the decay. The variation in the cone angle with concentration also implies (through eq 5) that the restricted diffusion constant, D_c, for angular motion within the cone becomes larger as the concentration of salt is reduced (Table 3).

The frequency dependence of the cone angles is shown in Figure 7 for LiBr and LiCl over five concentrations. The lines through the cone angles are linear fits, which capture the frequency dependence. The slopes from the linear fits, shown in Figure 8, decrease as the concentration decreased. Aside from the highest concentration, the slopes are identical within error for the two salts solutions. This implies that the ionic structuring probed through the frequency dependence of the cone angles is very similar for the two salt solutions and is changing in the same manner as the concentration of water is increased. For 1−10 and 1−16 concentrations, the cone angles are close to frequency-independent, with the fits giving very small slopes.

Figures 4 and 5 display LAS for some of the LiBr and LiCl concentrations. The spectra for concentrations that are not shown look similar. The LAS show that the high frequency side of the total absorption spectrum is dominated by the ODs H-bonded to halide anions (ODHal), while the low frequency side of the line has substantial contribution from OD bound to

https://doi.org/10.1021/acs.jpcb.2c08792
J. Phys. Chem. B 2023, 127, 4532−4543

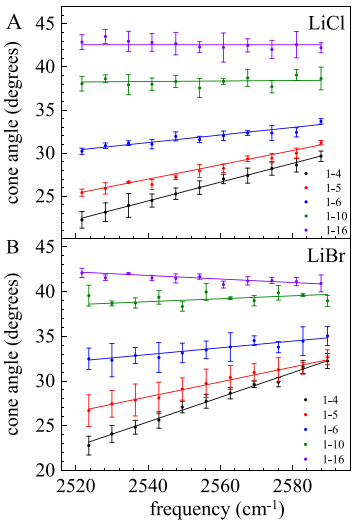

Figure 7. Cone angles from the wobbling-in-a-cone analysis of the frequency-dependent anisotropy decays for HOD in aqueous (A) LiCl solutions and (B) LiBr solutions. The solid lines are linear fits. Error bars are the standard deviation of experiments on three samples for each measured concentration.

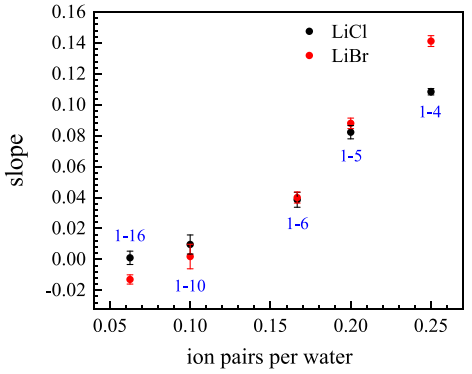

Figure 8. Slopes of frequency-dependent cone angles as a function of salt concentration. Slopes determined from the linear fits to the frequency-dependent cone angles at each concentration shown in Figure 7.

a water oxygen (ODO). As discussed above, the ODO spectrum at the highest salt concentrations is shifted to lower frequency than the ODO spectrum in pure water. The cone angles were measured between ~2520 and 2590 cm^{-1}. Over most of this range, there is substantial overlap of the ODHal and ODO spectra, with an increasing contribution from the ODO spectrum as the frequency decreases. The OD stretch frequency is determined by the species the OD is bound to, but the cone angle will be determined by the flexibility of all of the interacting species that associated with HOD.

As the concentration of water is increased from 1−4, to 1−5, to 1−6, there are more waters available to come closer to fully solvating the ions. The spectra of the many types of water ion clusters substantially overlap. The LAS does not strongly reflect a change in the distribution of these groupings. The spectra show a small relative change, with an increase in ODO H-bonding and a decrease in ODHal H-bonding. The spectra of ODOs in which Li^+ ions are bound or not bound to the OD oxygen strongly overlap. Because of the overlap of the 1−2 transition with the red side of the 0−1 transition, details of a shift in the lowest frequency absorbers are obscured. While the LAS barely show a change with concentration for the highest concentrations, the change in the slope of the cone angles with concentration (Figures 7 and 8) is substantial and an indicator that the distribution of ion/water configurations is changing. As the water concentration is increased, the slope decreases and the average cone angle increases. The smallest cone angles occurring at the lowest frequencies increases rapidly with increasing water concentrations. Thus, the most tightly structured configurations that can undergo the smallest angular sampling are disappearing, and on average, the networks of water and ions are becoming looser, sampling wider ranges of angles prior to relaxation of local structuring, which enable the final complete angular randomization. When the water concentration is 1−10 and 1−16, there is virtually no cone angle frequency dependence. As shown in Figure 4, the 1−16 LAS is very different from the high concentrations. The ODO band is, within experimental error, the same as pure water. The ODBr band has shifted slightly, ~4 cm^{-1}, to lower frequency. This shift may indicate fewer Li^+−Br^- ion pairs. At the higher water concentration, the Li^+ may tend toward being fully solvated by water rather than making ion pairs.

As can be seen in Figure 7, as the water concentration increases, the average cone angle increases. This trend shows that the ions, even at the higher water concentrations are still having a profound influence on the water orientational relaxation. In pure water, the anisotropy decay can be fit well with a single exponential with a 2.6 ps time constant. This is the time for complete orientational relaxation. The single exponential means there is no wobbling that requires constraint release to enable full orientational randomization. It is possible to fit the pure water $r(t)$ with a biexponential. When this is done, the first time constant is ~0.6 ps with very small amplitude, i.e., a very small cone angle. In either case, no cone or exceedingly small cone, data for the 1−16 concentration is clearly far from that of pure water. 1−16 is still a very high ion concentration, ~3.5 M of ion pairs, i.e., ~7 M of ions. As discussed below, ion pairs and some larger ion clusters are still present in the solution. At this concentration, there is insufficient water to screen the electric fields produced by nearby ions. At very low concentrations, <mM, the ions are electrostatically decoupled from each other and are randomly distributed in the water. At 3.5 M, the ions will not have random configurations and the water will experience significant electric fields. The water dipoles will interact with the local E field. Such interactions may provide a constraint on complete orientational relaxation but permit wobbling through a wide angular range.

Additional information can be gained from recent simulations.[57] All-atom molecular dynamics simulations of concentrated aqueous LiCl solutions reported the number of water-solvated ion pairs and large ion−water complexes for a wide range of concentrations (0.11 to 19.28 molal).[57] Radial distribution functions (RDFs) were calculated for Li^+-Cl^- as a function of concentration. It was found that the RDFs obtained from the MD simulations compared favorably with X-ray and neutron scattering experiments. The RDF information enabled the calculation of the fractions of Li^+ ions incorporated in ion complexes and the sorting of the ion complexes into different sizes at each LiCl concentration. The ion complexes were divided into contact ion pairs and larger ion complexes, which contained three or more ions.

Figure 9 shows the fractions determined from the simulations that are water solvated ion pairs and larger ion−

https://doi.org/10.1021/acs.jpcb.2c08792
J. Phys. Chem. B 2023, 127, 4532−4543

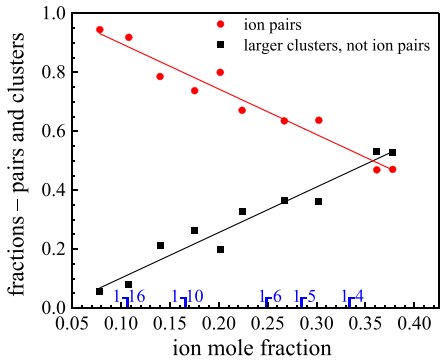

Figure 9. Fractions determined from the simulations[57] that are contact ion pair/water structures (red points) and larger ion-water clusters (black points) vs ion mole fraction. (Note that here, ion means all ions, so one LiCl is two ions.) The 1-N designations (1 ion pair per N water molecules) for the five samples' frequency-dependent cone angles plotted in Figure 7 are also shown. The lines are fits to the simulation data.

water clusters vs ion mole fraction. (Note that here ion means all ions, so one LiCl is two ions.) The designations for the five samples' frequency-dependent cone angles plotted in Figure 7 are also indicated. As the ion mole fraction decreases, the fraction of all ion clusters that are ion pairs increases and the fraction of large clusters decreases. The slope of the frequency-dependent cone angles becomes essentially zero at an ion mole fraction of ∼0.17 (1−10). This occurs when the large cluster fraction has decreased to ∼0.2 and the ion pair fraction has increased to ∼0.8. The comparison of the concentration dependences of the ion cluster fractions and the cone angle slopes suggests that the large clusters give rise to a greater diversity of water environments that determine the cone angles relative to the water solvating ion pairs. As the fraction of large clusters decreases with the concomitant increase in ion pairs, the reduction in range of water environment results in the decrease in the slope of the cone angles with frequency. In addition, as the fraction of large clusters decreases with decreasing ion concentration, the average cone angle becomes larger, suggesting that the large clusters constrain the angular range more than the ion pairs.

As the water concentration continues to increase past 1−16, the cone angle must go zero in the limit of pure water. One possibility is that the cone angle becomes larger and larger until the cone half angle is 180°, and the "cone" is now all angles, i.e., there is no longer a cone but rather complete sampling of the angular space. While only experiments can determine if this ever widening cone scenario is correct, it seems unlikely. To reach the 180° limit, at some point, the cone half angle would have to be very large but not 180°, e.g., 140°. That would be a full cone of 280°. To have such a cone, there would have to be constraints on the angular motions that permitted such a wide angle but no more. Thus, on average, the water molecules would sample almost all of the possible angular space in θ and φ and then have what amounts to a barrier that blocks further change in angle from the original orientation. Another possibility is that as the water concentration is increased, at some point, the increase in cone angle shown in Figure 7 turns around and tends toward zero. Future experiments will determine if there is a continuous increase in cone angle or if at some concentration the cone angle begins to decrease and decreases to zero at sufficiently low ion concentration. If the cone angle does decrease at some point, it will be very informative to observe the concentration at which the decrease begins.

4. CONCLUDING REMARKS

To investigate ion-dependent and concentration effects of ion/water H-bond networks at very high salt concentrations, we examined both LiCl and LiBr salt solutions using linear IR absorption spectroscopy and nonlinear IR experiments, i.e., PSPP spectroscopy. These experiments provided a substantial amount of information on the structure and dynamics of water in the presence of extensive ion pairing and clustering. We identified both general and anion specific effects of the ion/water network dynamics by examining these two salt solutions as a function of concentration.

In the experiments, we employed the OD stretch of dilute HOD in the ion/water solutions as the vibrational probe. Using the PSPP experiments to measure the frequency-dependent vibrational excited-state population relaxation, we were able to obtain Lifetime Amplitude Spectra. The LAS are the spectra of OD H-bonded to halide anions and OD H-bonded to water oxygens (see Figures 4 and 5). These spectra are not resolved in the linear FT-IR spectra due to the relatively small frequency shift. The areas of the two spectra, normalized to the total LAS spectrum, gave reasonable estimates of the ratios of hydroxyls bound to anions and water (see Table 2). At the highest concentrations of ions (1−4 to 1−7), the ratios of hydroxyls bound to halides and hydroxyls bound to water oxygens, ∼3, did not change a great deal with concentration, with far more hydroxyls bound to halides than to water. However, at lower ion concentration, 1−10, the ratio is 1. At 1−16 (∼3.5 M ion pairs), there were far more hydroxyls bound to water molecules than to halides.

The PSPP experiments also provided detailed information on water (HOD) orientational relaxation (see Figures 6−8). The time for complete randomization of the orientation was somewhat faster in LiBr solutions (9 ps) than in LiCl solutions (11 ps). Remarkably, the time for complete randomization, i.e., the slowest component of the anisotropy decay, is concentration-independent for both solutions, from ion pair-water concentrations of 1−4 to 1−16.

On a shorter time scale (∼2 ps), the anisotropy decay was caused by restricted orientational relaxation, i.e., wobbling-in-a-cone dynamics, in which the hydroxyls (OD) can sample only a limited range of angles. At the highest concentrations, 1−4 through 1−6, in both LiCl and LiBr solutions, the cone angles, which are the range of angles sampled prior to constraint release followed by complete angular sampling, have a substantial frequency dependence. As the frequency decreases, the cone angles become smaller. The frequency dependence is fit well by lines (see Figure 7). The slopes of the lines (see Figure 8) become smaller as the concentration of water is increased. By an ion pair-water concentration of 1−10, the slope is essentially zero. The high concentration frequency dependence shows that the water molecules are located in substantially different environments, which determine the frequency of the OD stretch. The OD stretch frequency will be strongly influenced by the H-bond strength but also by other local structural factors, e.g., whether or not a Li^+ cation is bound to the HOD oxygen lone pair. As the slope becomes smaller and eventually vanishes with increasing water concentration, the cone angle averaged over frequency becomes larger. The addition of water gives the water

https://doi.org/10.1021/acs.jpcb.2c08792
J. Phys. Chem. B 2023, 127, 4532−4543

molecules more angular freedom, implying overall less tightly packed environments.

The results leads to an intriguing general observation. As the concentration of ions drops from extremely high, 1 ion pair per 4 water molecules, to very high, 1 ion per 16 water molecule molecules, the dynamical properties are not approaching those of pure water. Four water molecules have 8 hydroxyls and 4 oxygens, which are not sufficient to solvate the Li^+ or the halide anions. Sixteen water molecules have 32 hydroxyl and 16 oxygens. In dilute solution, a variety of results indicate that it takes 6 to 8 hydroxyls to solvate Cl^- or Br^- and 4 oxygens to solvate a lithium cation. The concentration, 1−16, is still very high, but at this concentration, there are sufficient hydroxyls and oxygens to solvate the ions and have some water−water network. The experimental results show that the dynamical properties, which imply the structure properties, are moving away from those of pure water. The average restricted orientational cone angles are large and becoming larger as the water concentration increases, in contrast to pure water which has an extremely small or no orientational cone. It will provide a good deal of insight to extend these experiments to lower concentrations to find the turnover concentration and to study other salt solutions to see if they display dynamical properties that are analogous to the lithium salts studied here.

AUTHOR INFORMATION

Corresponding Author

Michael D. Fayer − *Department of Chemistry, Stanford University, Stanford, California 94305, United States;* orcid.org/0000-0002-0021-1815; Phone: (650) 723-4446; Email: fayer@stanford.edu

Authors

Sean A. Roget − *Department of Chemistry, Stanford University, Stanford, California 94305, United States;* orcid.org/0000-0003-2470-3571

Tristan R. Heck − *Department of Chemistry, Stanford University, Stanford, California 94305, United States;* orcid.org/0000-0002-7605-1555

Kimberly A. Carter-Fenk − *Department of Chemistry, Stanford University, Stanford, California 94305, United States;* orcid.org/0000-0003-0071-7127

Complete contact information is available at: https://pubs.acs.org/10.1021/acs.jpcb.2c08792

Notes

The authors declare no competing financial interest.

ACKNOWLEDGMENTS

We would like to thank Professor Ward Thompson, University of Kansas, and Stephen van Wyck, Stanford University, for very helpful discussions. This work was supported by the National Science Foundation, Division of Chemistry, Award Number 1954392. K.A.C.-F. is supported by a Stanford Science Fellowship.

REFERENCES

(1) Eisenberg, D.; Kauzmann, W. *The Structure and Properties of Water*. Oxford University Press: 2005, DOI: 10.1093/acprof:oso/9780198570264.001.0001.

(2) Bernal, J. D.; Fowler, R. H. A Theory of Water and Ionic Solution, with Particular Reference to Hydrogen and Hydroxyl Ions. *J. Chem. Phys.* **1933**, *1*, 515−548.

(3) Prendergast, D.; Galli, G. X-Ray Absorption Spectra of Water from First Principles Calculations. *Phys. Rev. Lett.* **2006**, *96*, No. 215502.

(4) Asbury, J. B.; Steinel, T.; Stromberg, C.; Corcelli, S. A.; Lawrence, C. P.; Skinner, J. L.; Fayer, M. D. Water Dynamics: Vibrational Echo Correlation Spectroscopy and Comparison to Molecular Dynamics Simulations. *J. Phys.Chem. A* **2004**, *108*, 1107−1119.

(5) Steinel, T.; Asbury, J. B.; Corcelli, S. A.; Lawrence, C. P.; Skinner, J. L.; Fayer, M. D. Water Dynamics: Dependence on Local Structure Probed with Vibrational Echo Correlation Spectroscopy. *Chem. Phys. Lett.* **2004**, *386*, 295−300.

(6) Park, S.; Fayer, M. D. Hydrogen Bond Dynamics in Aqueous Nabr Solutions. *Proc. Natl. Acad. Sci. U. S. A.* **2007**, *104*, 16731−16738.

(7) Rezus, Y. L. A.; Bakker, H. J. On the Orientational Relaxation of Hdo in Liquid Water. *J. Chem. Phys.* **2005**, *123*, 114502.

(8) Ohtaki, H.; Radnai, T. Structure and Dynamics of Hydrated Ions. *Chem. Rev.* **1993**, *93*, 1157−1204.

(9) Soper, A. K.; Weckström, K. Ion Solvation and Water Structure in Potassium Halide Aqueous Solutions. *Biophys. Chem.* **2006**, *124*, 180−191.

(10) Powell, D. H.; Neilson, G. W.; Enderby, J. E. The Structure of Cl- in Aqueous Solution: An Experimental Determination of G(ClH)(R) and G(ClO)(R). *J. Phys.: Condens. Matter* **1993**, *5*, 5723−5730.

(11) Tielrooij, K. J.; van der Post, S. T.; Hunger, J.; Bonn, M.; Bakker, H. J. Cooperativity in Ion Hydration. *J. Phys. Chem. B* **2011**, *115*, 12638−12647.

(12) Endom, L.; Hertz, H. G.; Thül, B.; Zeidler, M. D. A Microdynamic Model of Electrolyte Solutions as Derived from Nuclear Magnetic Relaxation and Self-Diffusion Data. *Ber. Bunsen. Phys. Chem.* **1967**, *71*, 1008−1031.

(13) Giammanco, C. H.; Wong, D. B.; Fayer, M. D. Water Dynamics in Divalent and Monovalent Concentrated Salt Solutions. *J. Phys. Chem. B* **2012**, *116*, 13781−13792.

(14) Post, S. T. v. d.; Bakker, H. J. The Combined Effect of Cations and Anions on the Dynamics of Water. *Phys. Chem. Chem. Phys.* **2012**, *14*, 6280−6288.

(15) Roget, S. A.; Carter-Fenk, K. A.; Fayer, M. D. Water Dynamics and Structure of Highly Concentrated Licl Solutions Investigated Using Ultrafast Infrared Spectroscopy. *J. Am. Chem. Soc.* **2022**, *144*, 4233−4243.

(16) Laage, D.; Stirnemann, G.; Sterpone, F.; Rey, R.; Hynes, J. T. Reorientation and Allied Dynamics in Water and Aqueous Solutions. *Annu. Rev. Phys. Chem.* **2011**, *62*, 395−416.

(17) Stirnemann, G.; Wernersson, E.; Jungwirth, P.; Laage, D. Mechanisms of Acceleration and Retardation of Water Dynamics by Ions. *J. Am. Chem. Soc.* **2013**, *135*, 11824−11831.

(18) Pluhařová, E.; Stirnemann, G.; Laage, D. On Water Reorientation Dynamics in Cation Hydration Shells. *J. Mol. Liq.* **2022**, *363*, No. 119886.

(19) Suo, L.; Borodin, O.; Gao, T.; Olguin, M.; Ho, J.; Fan, X.; Luo, C.; Wang, C.; Xu, K. "Water-in-Salt"; Electrolyte Enables High-Voltage Aqueous Lithium-Ion Chemistries. *Science* **2015**, *350*, 938−943.

(20) Yamada, Y.; Usui, K.; Sodeyama, K.; Ko, S.; Tateyama, Y.; Yamada, A. Hydrate-Melt Electrolytes for High-Energy-Density Aqueous Batteries. *Nat. Energy* **2016**, *1*, 16129.

(21) Li, M.; Wang, C.; Chen, Z.; Xu, K.; Lu, J. New Concepts in Electrolytes. *Chem. Rev.* **2020**, *120*, 6783−6819.

(22) Lewis, N. H. C.; Zhang, Y.; Dereka, B.; Carino, E. V.; Maginn, E. J.; Tokmakoff, A. Signatures of Ion Pairing and Aggregation in the Vibrational Spectroscopy of Super-Concentrated Aqueous Lithium Bistriflimide Solutions. *J. Phys. Chem. C* **2020**, *124*, 3470−3481.

(23) Lim, J.; Park, K.; Lee, H.; Kim, J.; Kwak, K.; Cho, M. Nanometric Water Channels in Water-in-Salt Lithium Ion Battery Electrolyte. *J. Am. Chem. Soc.* **2018**, *140*, 15661−15667.

(24) Jeon, J.; Lee, H.; Choi, J.-H.; Cho, M. Modeling and Simulation of Concentrated Aqueous Solutions of Litfsi for Battery Applications. *J. Phys. Chem. C* **2020**, *124*, 11790−11799.
(25) Bergstroem, P.-A.; Lindgren, J.; Kristiansson, O. An Ir Study of the Hydration of Clo_4^-, No_3^-, I^-, Br^-, Cl^-, and So_4^{2-} Anions in Aqueous Solution. *J. Phys. Chem.* **1991**, *95*, 8575−8580.
(26) Kropman, M. F.; Bakker, H. J. Vibrational Relaxation of Liquid Water in Ionic Solvation Shells. *Chem. Phys. Lett.* **2003**, *370*, 741−746.
(27) Kinosita, K.; Kawato, S.; Ikegami, A. Theory of Fluorescence Polarization Decay in Membranes. *Biophys. J.* **1977**, *20*, 289−305.
(28) Lipari, G.; Szabo, A. Effect of Librational Motion on Fluorescence Depolarization and Nuclear Magnetic-Resonance Relaxation in Macromolecules and Membranes. *Biophys. J.* **1980**, *30*, 489−506.
(29) Wang, C. C.; Pecora, R. Time-Correlation Functions for Restricted Rotational Diffusion. *J. Chem. Phys.* **1980**, *72*, 5333−5340.
(30) Kinosita, K.; Ikegami, A.; Kawato, S. On the Wobbling-in-Cone Analysis of Fluorescence Anisotropy Decay. *Biophys. J.* **1982**, *37*, 461−464.
(31) Hare, D. E.; Sorensen, C. M. Raman Spectroscopic Study of Dilute Hod in Liquid H2o in the Temperature Range − 31.5 to 160 °C. *J. Chem. Phys.* **1990**, *93*, 6954−6961.
(32) Woutersen, S.; Bakker, H. J. Resonant Intermolecular Transfer of Vibrational Energy in Liquid Water. *Nature* **1999**, *402*, 507−509.
(33) Corcelli, S.; Lawrence, C. P.; Skinner, J. L. Combined Electronic Structure/Molecular Dynamics Approach for Ultrafast Infrared Spectroscopy of Dilute Hod in Liquid H2o and D2o. *J. Chem. Phys.* **2004**, *120*, 8107−8117.
(34) Fenn, E. E.; Wong, D. B.; Fayer, M. D. Water Dynamics in Small Reverse Micelles in Two Solvents: Two-Dimensional Infrared Vibrational Echoes with Two-Dimensional Background Subtraction. *J. Chem. Phys.* **2011**, *134*, No. 054512.
(35) Steinel, T.; Asbury, J. B.; Zheng, J. R.; Fayer, M. D. Watching Hydrogen Bonds Break: A Transient Absorption Study of Water. *J. Phys. Chem. A* **2004**, *108*, 10957−10964.
(36) Park, S.; Moilanen, D. E.; Fayer, M. D. Water Dynamics-the Effects of Ions and Nanoconfinement. *J. Phys. Chem. B* **2008**, *112*, 5279−5290.
(37) Bian, H.; Chen, H.; Zhang, Q.; Li, J.; Wen, X.; Zhuang, W.; Zheng, J. Cation Effects on Rotational Dynamics of Anions and Water Molecules in Alkali (Li^+, Na^+, K^+, Cs^+) Thiocyanate (Scn−) Aqueous Solutions. *J. Phys. Chem. B* **2013**, *117*, 7972−7984.
(38) Badger, R. M.; Bauer, S. H. Spectroscopic Studies of the Hydrogen Bond. *J. Chem. Phys.* **1937**, *5*, 839−851.
(39) Smiechowski, M.; Gojło, E.; Stangret, J. Ionic Hydration in Lipf6, Napf6, and Kpf6 Aqueous Solutions Derived from Infrared Hdo Spectra. *J. Phys. Chem. B* **2004**, *108*, 15938−15943.
(40) Moilanen, D. E.; Wong, D.; Rosenfeld, D. E.; Fenn, E. E.; Fayer, M. D. Ion-Water Hydrogen-Bond Switching Observed with 2D IR Vibrational Echo Chemical Exchange Spectroscopy. *Proc. Natl. Acad. Sci. U. S. A.* **2009**, *106*, 375−380.
(41) Giammanco, C. H.; Kramer, P. L.; Fayer, M. D. Ionic Liquid Versus Li+ Aqueous Solutions: Water Dynamics near Bistriflimide Anions. *J. Phys. Chem. B* **2016**, *120*, 9997−10009.
(42) Schmidt, J. R.; Corcelli, S. A.; Skinner, J. L. Pronounced Non-Condon Effects in the Ultrafast Infrared Spectroscopy of Water. *J. Chem. Phys.* **2005**, *123*, No. 044513(13).
(43) Loparo, J. J.; Roberts, S. T.; Nicodemus, R. A.; Tokmakoff, A. Variation of the Transition Dipole Moment across the Oh Stretching Band of Water. *Chem. Phys.* **2007**, *341*, 218−229.
(44) Bakker, H. J. Structural Dynamics of Aqueous Salt Solutions. *Chem. Rev.* **2008**, *108*, 1456−1473.
(45) Moilanen, D. E.; Fenn, E. E.; Wong, D.; Fayer, M. D. Water Dynamics in Large and Small Reverse Micelles: From Two Ensembles to Collective Behavior. *J. Chem. Phys.* **2009**, *131*, No. 014704.
(46) Yamada, S. A.; Hung, S. T.; Shin, J. Y.; Fayer, M. D. Complex Formation and Dissociation Dynamics on Amorphous Silica Surfaces. *J. Phys. Chem. B* **2021**, *125*, 4566−4581.
(47) Kenkre, V. M.; Tokmakoff, A.; Fayer, M. D. Theory of Vibrational Relaxation of Polyatomic Molecules in Liquids. *J. Chem. Phys.* **1994**, *101*, 10618−10629.
(48) Wong, D. B.; Giammanco, C. H.; Fenn, E. E.; Fayer, M. D. Dynamics of Isolated Water Molecules in a Sea of Ions in a Room Temperature Ionic Liquid. *J. Phys. Chem. B* **2012**, *117*, 623−635.
(49) Kramer, P. L.; Giammanco, C. H.; Fayer, M. D. Dynamics of Water, Methanol, and Ethanol in a Room Temperature Ionic Liquid. *J. Chem. Phys.* **2015**, *142*, 212408.
(50) Yan, C.; Nishida, J.; Yuan, R.; Fayer, M. D. Water of Hydration Dynamics in Minerals Gypsum and Bassanite: Ultrafast 2D IR Spectroscopy of Rocks. *J. Am. Chem. Soc.* **2016**, *138*, 9694−9703.
(51) Moilanen, D. E.; Fenn, E. E.; Wong, D.; Fayer, M. D. Water Dynamics at the Interface in Aot Reverse Micelles. *J. Phys. Chem. B* **2009**, *113*, 8560−8568.
(52) Zeng, Y.; Jia, Y.; Yan, T.; Zhuang, W. Binary Structure and Dynamics of the Hydrogen Bonds in the Hydration Shells of Ions. *Phys. Chem. Chem. Phys.* **2021**, *23*, 11400−11410.
(53) Auer, B.; Kumar, R.; Schmidt, J. R.; Skinner, J. L. Multidimensional Ultrafast Spectroscopy Special Feature: Hydrogen Bonding and Raman, Ir, and 2d-Ir Spectroscopy of Dilute Hod in Liquid D2o. *Proc. Natl. Acad. Sci. U. S. A.* **2007**, *104*, 14215−14220.
(54) Boyer, M. A.; Marsalek, O.; Heindel, J. P.; Markland, T. E.; McCoy, A. B.; Xantheas, S. S. Beyond Badger's Rule: The Origins and Generality of the Structure−Spectra Relationship of Aqueous Hydrogen Bonds. *J. Phys. Chem. Lett.* **2019**, *10*, 918−924.
(55) Antalek, M.; Pace, E.; Hedman, B.; Hodgson, K. O.; Chillemi, G.; Benfatto, M.; Sarangi, R.; Frank, P. Solvation Structure of the Halides from X-Ray Absorption Spectroscopy. *J. Chem. Phys.* **2016**, *145*, No. 044318.
(56) Ibuki, K.; Bopp, P. A. Molecular Dynamics Simulations of Aqueous Licl Solutions at Room Temperature through the Entire Concentration Range. *J. Mol. Liq.* **2009**, *147*, 56−63.
(57) Singh, M. B.; Dalvi, V. H.; Gaikar, V. G. Investigations of Clustering of Ions and Diffusivity in Concentrated Aqueous Solutions of Lithium Chloride by Molecular Dynamic Simulations. *RSC Adv.* **2015**, *5*, 15328−15337.
(58) Pethes, I. The Structure of Aqueous Lithium Chloride Solutions at High Concentrations as Revealed by a Comparison of Classical Interatomic Potential Models. *J. Mol. Liq.* **2018**, *264*, 179−197.
(59) Eaves, J. D.; Loparo, J. J.; Fecko, C. J.; Roberts, S. T.; Tokmakoff, A.; Geissler, P. L. Hydrogen Bonds in Liquid Water Are Broken Only Fleetingly. *Proc. Natl. Acad. Sci. U. S. A.* **2005**, *102*, 13019−13022.
(60) Carr, J. K.; Buchanan, L. E.; Schmidt, J. R.; Zanni, M. T.; Skinner, J. L. Structure and Dynamics of Urea/Water Mixtures Investigated Byvibrational Spectroscopy and Molecular Dynamics Simulation. *J. Phys. Chem. B* **2013**, *117*, 13291−13300.
(61) Palchowdhury, S.; Mukherjee, K.; Maroncelli, M. Rapid Water Dynamics Structures the Oh-Stretching Spectra of Solitary Water in Ionic Liquids and Dipolar Solvents Editors-Pick. *J. Chem. Phys.* **2022**, *157*, No. 084502.
(62) Mukherjee, K.; Palchowdhury, S.; Maroncelli, M. Oh Stretching and Libration Bands of Solitary Water in Ionic Liquids and Dipolar Solvents Share a Single Dependence on Solvent Polarity. *J. Phys. Chem. B* **2022**, *126*, 4584−4598.
(63) Debye, P. J. W. *Polar Molecules*. Dover Publications: New York, 1928; p 172.
(64) Laage, D.; Hynes, J. T. A Molecular Jump Mechanism of Water Reorientation. *Science* **2006**, *311*, 832−835.
(65) Laage, D.; Hynes, J. T. Reorientional Dynamics of Water Molecules in Anionic Hydration Shells. *Proc. Nat. Acad. Sci.* **2007**, *104*, 11167−11172.
(66) Laage, D.; Elsaesser, T.; Hynes, J. T. Water Dynamics in the Hydration Shells of Biomolecules. *Chem. Rev.* **2017**, *117*, 10694−10725.
(67) Moilanen, D. E.; Fenn, E. E.; Lin, Y. S.; Skinner, J. L.; Bagchi, B.; Fayer, M. D. Water Inertial Reorientation: Hydrogen Bond

https://doi.org/10.1021/acs.jpcb.2c08792
J. Phys. Chem. B 2023, 127, 4532−4543

Strength and the Angular Potential. *Proc. Nat. Acad. Sci.* **2008**, *105*, 5295−5300.
(68) Tan, H.-S.; Piletic, I. R.; Fayer, M. D. Orientational Dynamics of Water Confined on a Nanometer Length Scale in Reverse Micelles. *J. Chem. Phys.* **2005**, *122*, 174501.

https://doi.org/10.1021/acs.jpcb.2c08792
J. Phys. Chem. B 2023, 127, 4532−4543